J|A|C|S
ARTICLES
Published on Web 01/29/2003

Understanding the Correlation of Structure and Selectivity in the Chiral-Phosphoramide-Catalyzed Enantioselective Allylation Reactions: Solution and Solid-State Structural Studies of Bisphosphoramide·$SnCl_4$ Complexes

Scott E. Denmark* and Jiping Fu

Contribution from the Roger Adams Laboratory, Department of Chemistry, University of Illinois, Urbana, Illinois 61801

Received October 17, 2002; E-mail: denmark@scs.uiuc.edu

Abstract: Complexation of bisphosphoramides, linked by various length methylene tethers, with tin tetrachloride was studied by both solution NMR spectroscopy and single-crystal X-ray crystallography. The formation of *cis*-configured, octahedral 1/1 bisphosphoramide·$SnCl_4$ complexes was supported by both crystallographic and solution NMR studies. In addition, the formation of such complexes was shown to be highly dependent on the tether length and solution concentration. Single-crystal X-ray analysis of bisphosphoramide·$SnCl_4$ complexes also provided detailed information on the stereochemical environment relevant to the enantioselectivity of asymmetric allylation reactions.

Introduction

The invention and development of catalytic enantioselective reactions are among the most challenging and intensively studied frontiers in organic synthesis.[1] In these reactions, chiral ligands are often utilized to modulate the asymmetric environment of the metal reaction centers and to promote asymmetric induction. Thus, understanding the coordination environment of the chiral ligand/metal center complexes is crucial for the rational development of highly selective catalysts. To achieve such understanding, solution spectroscopy and solid-state X-ray analysis of the ligand/metal complexes are the most powerful and useful tools.[2]

Background

Over the past decade, the chemistry of chiral phosphoramides[3,4] as catalysts in combination with organotrichlorosilanes has been extensively developed in these laboratories.[5−7] The concept and mechanism of such an activation, as illustrated in the chiral-phosphoramide-catalyzed allylation, are shown in Scheme 1.[6,8] The addition of allyltrichlorosilanes **1** to aldehydes **2** is promoted by chiral phosphoramides to give chiral, nonracemic homoallylic alcohols **3** with high diastereocontrol (Scheme 1). In the reaction promoted by **4** (Chart 1), kinetic studies revealed that the reaction involves two molecules of the phosphoramide in the transition structure.[6a,b] Thus, binding two catalyst molecules (LB) induces ionization of chloride anion, and the allylation proceeds, after coordination of aldehyde, through a hexacoordinate cationic silicon assembly (Figure 1).

Scheme 1

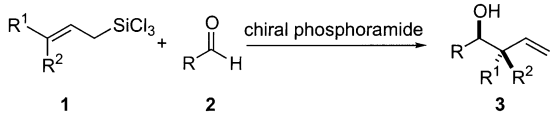

1 **2** **3**

(1) *Comprehensive Asymmetric Catalysis*; Jacobsen, E. N., Pfaltz, A., Yamamoto, H., Eds.; Springer-Verlag: Heidelberg, 1999; Vols. I−III.
(2) (a) Shambayati, S.; Crowe, W. E.; Schreiber, S. L. *Angew. Chem., Int. Ed. Engl.* **1990**, *29*, 256. (b) Seebach, D. *Angew. Chem., Int. Ed. Engl.* **1988**, *27*, 1624. (c) Seebach, D.; Beck, A. K.; Heckel, A. *Angew. Chem., Int. Ed.* **2001**, *20*, 92. (d) Gaul, C.; Schweizer, B. W.; Seebach, D. *Helv. Chim. Acta* **2002**, *85*, 1546. (e) Boche, G. *Angew. Chem., Int. Ed. Engl.* **1989**, *28*, 277. (f) Ooi, T.; Maruoka, K. In *Modern Carbonyl Chemistry*; Otera, J., Ed.; Wiley-VCH: Weinheim, 2000; Chapter 1. (g) Saito, S.; Yamamoto, H. In *Modern Carbonyl Chemistry*; Otera, J., Ed.; Wiley-VCH: Weinheim, 2000; Chapter 2.
(3) General reference on the properties and the application of phosphoramides: (a) Normant, H. *Russ. Chem. Rev.* (*Engl. Transl.*) **1970**, *39*, 457. (b) Reichardt, C. *Solvents and Solvent Effects in Organic Chemistry*; VCH: Germany, 1988. (c) Luteri, G. F.; Ford, W. T. *J. Org. Chem.* **1977**, *42*, 820. (d) Gutmann, V. *The Donor-Acceptor Approach to Molecular Interactions*; Plenum: New York, 1978.
(4) Denmark, S. E.; Su, X.; Nishigaichi, Y.; Coe, D. M.; Wong, K.-T.; Winter, S. B. D.; Choi, J. Y. *J. Org. Chem.* **1999**, *64*, 1958.
(5) Chiral Lewis base-catalyzed aldol reaction: Denmark, S. E.; Stavenger, R. A. *Acc. Chem. Res.* **2000**, *33*, 432.
(6) Chiral-phosphoramide-catalyzed allylation reaction: (a) Denmark, S. E.; Coe, D. M.; Pratt, N. E.; Griedel, B. D. *J. Org. Chem.* **1994**, *59*, 6161. (b) Denmark, S. E.; Fu, J. *J. Am. Chem. Soc.* **2000**, *122*, 12021. (c) Denmark, S. E.; Fu, J. *J. Am. Chem. Soc.* **2001**, *123*, 9488. (d) Denmark, S. E.; Fu, J. *Org. Lett.* **2002**, *4*, 1951. (e) Denmark, S. E.; Fu, J. *Chem. Commun.* **2003**, 167.
(7) Reactions with $SiCl_4$: (a) Denmark, S. E.; Barsanti, P. A.; Wong, K.-T.; Stavenger, R. A. *J. Org. Chem.* **1998**, *63*, 2428. (b) Denmark, S. E.; Wynn, T.; Jellerichs, B. G. *Angew. Chem., Int. Ed.* **2001**, *40*, 2255. (c) Denmark, S. E.; Wynn, T. *J. Am. Chem. Soc.* **2001**, *123*, 6199. (d) Denmark, S. E.; Wynn, T.; Beutner, G. L. *J. Am. Chem. Soc.* **2002**, *124*, 13405.
(8) Reference on other chiral-Lewis-base-catalyzed enantioselective allylation reactions: (a) Iseki, K.; Kuroki, Y.; Takahashi, M.; Kobayashi, Y. *Tetrahedron Lett.* **1996**, *37*, 5149. (b) Iseki, K.; Kuroki, Y.; Takahashi, M.; Kishimoto, S.; Kobayashi, Y. *Tetrahedron* **1997**, *53*, 3513. (c) Hellwig, J.; Belser, T.; Muller, J. F. K. *Tetrahedron Lett.* **2001**, *42*, 5417. (d) Iseki, K.; Mizuno, S.; Kuroki, Y.; Kobayashi, Y. *Tetrahedron Lett.* **1998**, *39*, 2767. (e) Iseki, K.; Mizuno, S.; Kuroki, Y.; Kobayashi, Y. *Tetrahedron* **1999**, *55*, 977. (f) Nakajima, M.; Saito, M.; Shiro, M.; Hashimoto, S. *J. Am. Chem. Soc.* **1998**, *120*, 6419. (g) Malkov, A. V.; Orsini, M.; Pernazza, D.; Muir, K. W.; Langer, V.; Meghani, P.; Kocovsky, P. *Org. Lett.* **2002**, *4*, 1047. (h) Shimada, T.; Kina, A.; Ikeda, S.; Hayashi, T. *Org. Lett.* **2002**, *4*, 2799. (i) Chataigner, I.; Piarulli, U.; Gennari, C. *Tetrahedron Lett.* **1999**, *40*, 3633. (j) Angell, R. M.; Barrett, A. G. M.; Braddock, D. C.; Swallow, S.; Vickery, B. D. *Chem. Commun.* **1997**, 919.

10.1021/ja021280g CCC: $25.00

Chart 1

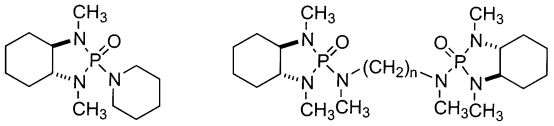

4

5a: n=2; **5b**: n=3; **5c**: n=4; **5d**: n=5; **5e**: n=6

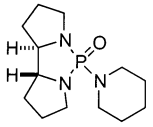

6

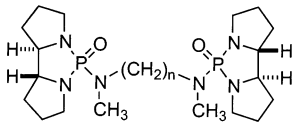

7c: n=4; **7d**: n=5; **7e**: n=6

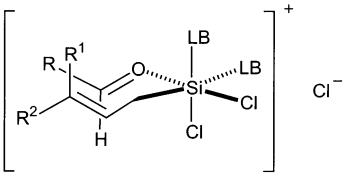

Figure 1. Transition structure assembly for allylation reactions (LB = Lewis base catalyst).

To increase the efficiency of the catalyst, we employed bisphosphoramides **5** (Chart 1) with the expectation of improving the reaction rate and selectivity by increasing the effective concentration of the second catalyst molecule through proximity.

In the addition of allyltrichlorosilane **1a** to benzaldehyde **2a** promoted by bisphosphoramides **5**, the enantiomeric composition of the product **3a** was found to be highly dependent on the tether length.[6b] As shown in Figure 2, nearly racemic product was obtained with **5a**. A dramatic increase in enantioselectivity was seen in the change from **5c** (er only 1.4/1) to **5d**, wherein the er was 5.7/1. The er decreased again to 2.7/1 when **5e** was used. Such dependence of reaction enantioselectivity on tether length was also observed in the reaction catalyzed by **7** with (*R*,*R*)-2,2′-bispyrrolidine.[6c] The enantioselective variation on the

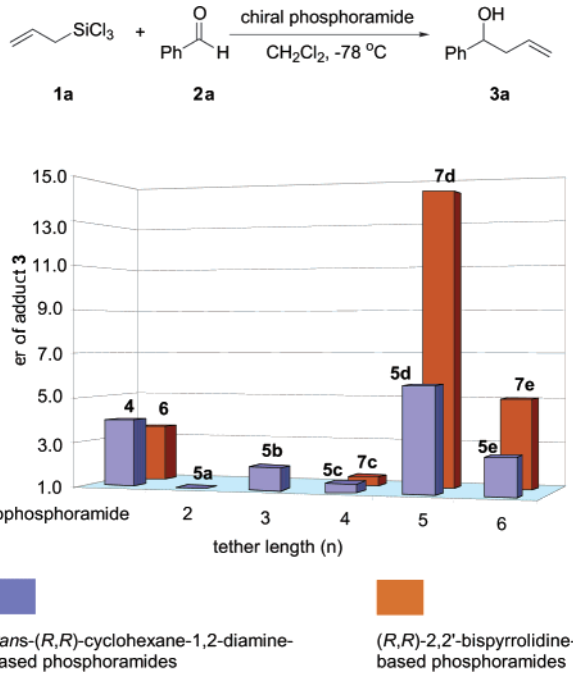

Figure 2. Dependence of allylation product ee on the tether length and chiral diamine backbone.

tether length followed the same trend as that seen with bisphosphoramide **5**. In this case, the enantioselectivity change from **7c** to **7d** was even more striking. Whereas **7c** gave only 1.4/1 er in the allylation reaction, **7d** (with a five-methylene tether) improved the er up to 14/1, which was also significantly higher than that obtained with bisphosphoramide **5d** derived from *trans*-(*R*,*R*)-cyclohexane-1,2-diamine.

Although the variation in selectivity was perplexing, these studies clearly demonstrated cooperativity between the two phosphoramide units. More importantly, the use of bisphosphoramides with a five-methylene-unit tether significantly improved the enantioselectivity as compared to that with monophosphoramides. The successful implementation of bisphosphoramides in the allylation reaction led us to apply bisphosphoramides in other reactions involving trichlorosilyl species such as the aldol addition or reactions with $SiCl_4$ (Scheme 2),[7c,d,9] in which the two-phosphoramide mechanistic pathway is also believed to be operative. In these reactions with bisphosphoramides **8** as catalysts, a pronounced effect of tether length on the product enantioselectivity was also observed. Moreover, the best enantioselectivities were uniformly achieved using the five-methylene-tethered bisphosphoramide **8d**.

Scheme 2

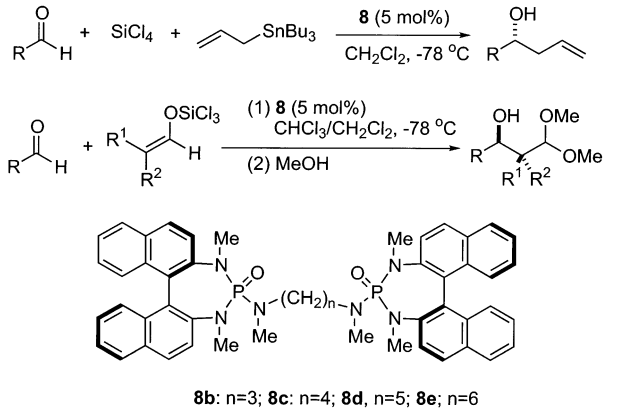

8b: n=3; **8c**: n=4; **8d**, n=5; **8e**; n=6

Our explanation for the strong cooperativity between the two phosphoramide units in these reactions involves chelation of the reactive silicon center by the bisphosphoramides in the transition structure. Thus, the restriction provided by the tether dictates the disposition of the phosphoramides, which in turn determines the coordination environment of the reaction centers.[10,11] However, considering the large ring sizes (9−13-membered rings, Figure 3) in the chelated bisphosphoramide·

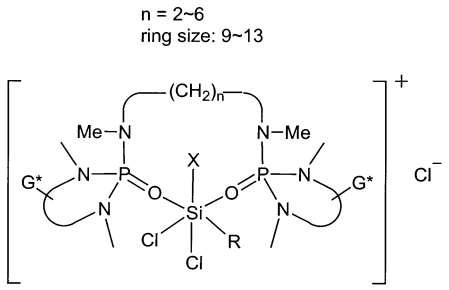

Figure 3. Hypothetical bisphosphoramide silicon complex.

(9) Denmark, S. E.; Ghosh, S. K. *Angew. Chem., Int. Ed.* **2001**, *40*, 4759.
(10) Another study on the operativity of dimeric catalysts tethered with methylene units: Konsler, R. G.; Karl, J.; Jacobsen, E. N. *J. Am. Chem. Soc.* **1998**, *120*, 10780.

silicon complexes, it was rather remarkable that subtle changes of the flexible methylene chain would have such profound effects.

To elucidate the relationship between the catalyst structure and its selectivity and reactivity as well as to provide guides for the design of better catalysts, it is necessary to have a clear understanding of the bisphosphoramide·Lewis acid complex structure. Unfortunately, the complexation of phosphoramides and chlorosilanes (e.g., $SiCl_4$) is very weak as judged by ^1H and ^{31}P NMR spectroscopy; thus, little information could be obtained. On the other hand, phosphoramides have been reported to bind strongly to $SnCl_4$ and to form hexacoordinate, 2/1, *cis*- or *trans*-complexes, both of which have been studied by X-ray crystallographic analysis.[12,13] The existence of these complexes in solution is also supported by the appearance of a triplet signal in the ^{119}Sn NMR spectrum due to coupling with the two $I = {}^1/_2$ ^{31}P nuclei (Figure 4). Furthermore, the chemical shift and coupling constant of the ^{119}Sn signal provided valuable information on the geometry of the two phosphoramides in the hexacoordinate tin complexes.[13,14] Generally, the *trans*-hexacoordinate complexes have higher coupling constants than the corresponding *cis*-complexes. For example, in the ^{119}Sn NMR spectrum of $(HMPA)_2$·$SnCl_4$, the *trans*-complex has a $^3J_{^{119}Sn-^{31}P}$ coupling constant of 167 Hz at −727 ppm, whereas the *cis*-complex shows a $^3J_{^{119}Sn-^{31}P}$ of 102 Hz at −719 ppm.

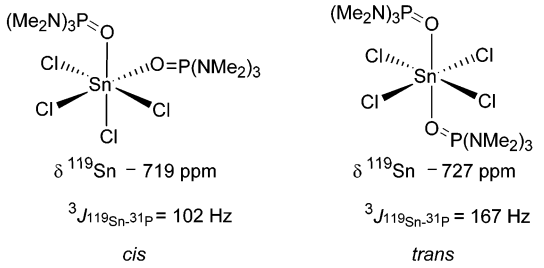

Figure 4. Spectroscopic data for *cis*- and *trans*-$(HMPA)_2$·$SnCl_4$ complexes.

Previous X-ray and NMR studies from these laboratories have provided a high level of structural detail on the complexation of chiral monophosphoramides with $SnCl_4$, which, in turn, provided the basis for understanding the selectivities of these catalysts in aldolization reactions.[13] The bisphosphoramides behave rather differently from the corresponding monophosphoramides, presumably due to consequences of chelation and the restriction of tether. To provide a structural basis for these observations, we undertook studies on the solution (NMR) and solid-state (X-ray) structure of bisphosphoramide·$SnCl_4$ complexes. In addition to the basic questions of composition and geometry of the complexes, we were most interested in learning about (1) the propensity of chelation as a function of tether length, (2) how the disposition of the phosphoramide unit changed in chelated complexes as a function of tether length, and (3) how we can understand the variation of enantioselectivity with tether length from these features.

(11) For a review on the ligand bite angle effect of the phosphine ligand: van Leeuwen, P. W. N. M.; Kamer, P. C. J.; Reek, J. N. H.; Dierkes, P. *Chem. Rev.* **2000**, *100*, 2741.
(12) Aslanov, L. A.; Ionov, V. M.; Attiya, V. M.; Permin, A. B.; Petrosyan, V. S. *Zh. Strukt. Khim.* **1977**, *18*, 1103.
(13) Denmark, S. E.; Su, X. *Tetrahedron* **1999**, *55*, 8727.
(14) (a) Ruzicka, S. J.; Favez, C. M. P.; Merbach, A. E. *Inorg. Chim. Acta* **1977**, *23*, 239. (b) Ruzicka, S. J.; Merbach, A. E. *Inorg. Chim. Acta* **1977**, *22*, 191. (c) Ruzicka, S. J.; Merbach, A. E. *Inorg. Chim. Acta* **1976**, *20*, 221.

Table 1. ^{119}Sn and ^{31}P Studies of Phosphoramide-$SnCl_4$ Complexation[a]

entry	phosphoramides	conc, M	^{119}Sn, ppm (mult, J (Hz))[b]	^{31}P NMR, ppm (J, Hz)[c]
1	**4** (2/1)[d]	0.20	−710 (t, 134)	25.2 (132)
			−722* (t, 196)[e]	26.2* (192)
2	**5a** ($n = 2$)	0.20	white precipitate formed	
3	**5a** ($n = 2$)	0.015	−722 (t, 182)	28.8 (177)
4	**5b** ($n = 3$)	0.20	−711 (t, 150)	27.3 (156)
			−725* (t, 192)	28.4* (188)
5	**5b** ($n = 3$)	0.015	−710 (t, 157)	27.3 (156)
6	**5c** ($n = 4$)	0.20	−712 (t, 141)	27.5 (140)
7	**5d** ($n = 5$)	0.20	−710 (t, 114)	28.4 (108)
8[f]	**5e** ($n = 6$)	0.20	−710 (t, 112)	29.1
			−724* (t, 208)	28.4*
9	**5e** ($n = 6$)	0.015	−712 (t, 113)	28.3 (110)
10	**7c** ($n = 4$)	0.20	−707 (t, 143)	21.0 (140)
11	**7d** ($n = 5$)	0.20	−704 (t, 112)	20.6 (112)
12	**7e** ($n = 6$)	0.20	−706 (t, 114)	many peaks
			−707 (t, 121)	
			−717 (t, 176)	

[a] The solutions were prepared under N_2 at room temperature with the indicated concentrations, and the NMR studies were carried out at room temperature as well. [b] "*" designates major peaks observed in the spectra. [c] The number in the parentheses is the coupling constant of the satellite signal; "*" designates major peaks observed in the spectra. [d] A solution of a 2/1 mixture of **4** and $SnCl_4$ was employed. [e] The ratio of the two peaks in the ^{119}Sn NMR spectrum is 1/2.1 (−710 and −722 ppm). [f] Satellites in the ^{31}P NMR are not clear due to overlap.

Results

1. NMR Spectroscopy. To examine the ability of bisphosphoramides to function as bidentate ligands and form hexacoordinate metal complexes in solution, we carried out solution ^{119}Sn and ^{31}P NMR spectroscopic studies. The solution samples for the spectroscopic studies were prepared by the addition of $SnCl_4$ to an equimolar amount of bisphosphoramides or 2 equiv of a monophosphoramide in $CDCl_3$ solution. The results of ^{119}Sn and ^{31}P NMR studies are collected in Table 1.

In general, in a 2/1 mixture of monophosphoramide and $SnCl_4$ or a 1/1 mixture of bisphosphoramide and $SnCl_4$, only triplet signals with chemical shifts ranging from −704 to −725 ppm were observed in the ^{119}Sn NMR spectra. The appearance of triplet signals suggested the coupling of two phosphorus atoms to the tin nucleus. The existence of phosphorus−tin coupling was also apparent by the ^{31}P NMR spectra in which two signals displaying ^{119}Sn satellites with the corresponding coupling constants were observed.

As was seen in the spectra of a 2/1 mixture of HMPA and $SnCl_4$, a 2/1 mixture of monophosphoramide **4** and $SnCl_4$ displayed two triplets in the ^{119}Sn NMR spectrum with coupling constants equal to 134 and 196 Hz (ratio of two signals = 1/2.1), indicating the presence of two species in solution. The species seen in the ^{119}Sn NMR spectra of 1/1 mixtures of bisphosphoramides and $SnCl_4$ were found to be highly dependent on the tether length and concentration. At 0.20 M concentration, a 1/1 mixture of **5a** and $SnCl_4$ resulted in the formation of a white precipitate, and little information could be obtained. In contrast, a sample prepared at low concentration (0.015 M) displayed a triplet with a coupling constant of 182 Hz in ^{119}Sn NMR spectrum. A 1/1 mixture of **5b** and $SnCl_4$ at 0.20 M concentration led to the formation of two triplet signals with coupling constants equal to 150 and 192 Hz, respectively. Most interestingly, only one triplet signal with a coupling constant equal to 157 Hz was observed when the complexation was performed

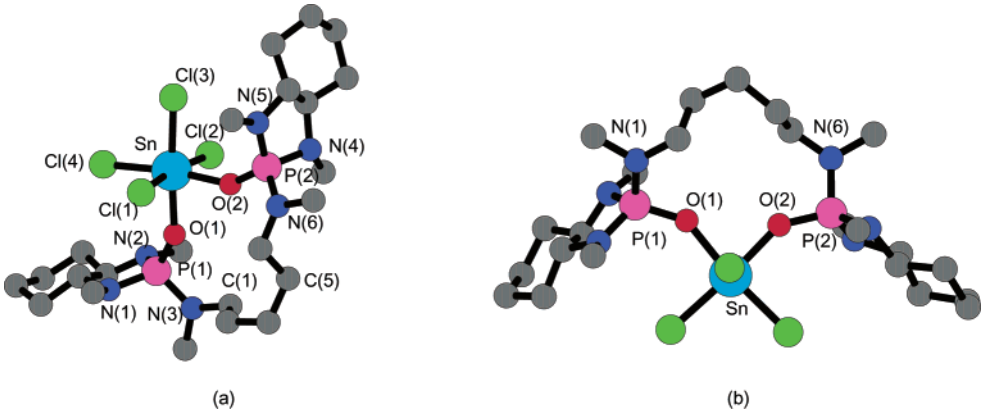

Figure 5. Chem 3D image of **5d**·$SnCl_4$ (hydrogens omitted for clarity).

at lower concentration (0.015 M) (entries 4 and 5, Table 1). The bisphosphoramide **5c** tethered with four methylene units behaved quite differently from **5a** and **5b**. A 1/1 mixture of **5c** and $SnCl_4$ at 0.20 M concentration displayed only one triplet with a coupling constant of 141 Hz in the ^{119}Sn NMR spectrum, suggesting the formation of a single species (entry 6). The exclusive formation of one species at 0.20 M concentration was also observed with an equimolar mixture of **5d** and $SnCl_4$, as suggested by the appearance of a single triplet with a coupling constant of 114 Hz (entry 7). The bisphosphoramide **5e** behaved similarly to **5b**. Thus, at higher concentration, the spectrum contained two triplets with coupling constants equal to 112 and 208 Hz, respectively, and only the triplet with a 113 Hz coupling constant was observed at lower concentration (entries 8 and 9, Table 1).

The ^{119}Sn spectra of the 1/1 bisphosphoramide·$SnCl_4$ complexes were not so dependent on the chiral diamine subunit. For example, an equimolar mixture of **7c** and $SnCl_4$ at 0.2 M shows only one triplet at −707 ppm, with the coupling constant equal to 143 Hz in the ^{119}Sn NMR spectrum. Similarly, only one triplet signal with a coupling constant of 112 Hz was observed in a 1/1 mixture of **7d** and $SnCl_4$ at 0.2 M concentration. Finally, a solution of a 1/1 mixture of **7e** and $SnCl_4$, however, displayed several triplet signals in the ^{119}Sn NMR spectrum (entry 12, Table 1).

These NMR studies clearly demonstrated that in the solutions containing equimolar amounts of bisphosphoramides and $SnCl_4$, different species were formed depending on the tether length and concentration, as suggested by the appearance of different signals in ^{119}Sn and ^{31}P NMR spectra. Among the phosphoramides employed, the bisphosphoramides **5c**, **5d**, **7c**, and **7d** with four or five methylene unit tethers were special in that a single species was formed at 0.20 M concentration.

2. X-ray Crystallography. To elucidate the constitution of the complexes formed in the solutions of **5** or **7** and $SnCl_4$, as well as to provide a clearer understanding of the effect of phosphoramide structure on the complexation, we next examined the solid-state structure of bisphosphoramide complexes with $SnCl_4$.

Thus, from a CH_2Cl_2 solution containing an equimolar of **5d** and $SnCl_4$, single crystals suitable for X-ray diffraction were obtained through slow diffusion of diethyl ether at −20 °C.

X-ray analysis of the complex revealed it to be a hexacoordinate complex of the formula **5d**·$SnCl_4$.[15a] As shown in Figure 5, the tin atom adopts an octahedral geometry, and **5d** chelates

Table 2. Selected Parameters for **5d**·$SnCl_4$, **7d**·$SnCl_4$, and **7c**·$SnCl_4$ Complexes[a]

parameter[b]	**5d**·$SnCl_4$	**7d**·$SnCl_4$	**7c**·$SnCl_4$
O(1)−Sn−O(2)	82.81(10)	84.87(13)	81.3(5)
∑N(1)	350.5(8)	349.5(10)	353.7(32)
∑N(2)	350.8(8)	354.4(9)	345.0(31)
∑N(3)	359.4(9)	359.1(9)	359.9(30)
O(1)−P(1)−N(3)−C(1)	2.3(4)	6.8(4)	19.4(16)
Sn−O(1)−P(1)	144.62(16)	140.99(15)	153.3(8)
Sn−O(1)−P(1)−N(3)	160.7(3)	−137.1(2)	−109.9(15)
distance N(3)−N(6)	5.805	5.752	4.754

[a] Because the two phosphoramide units in each complex are nearly identical, only one unit is depicted. [b] All angles in degrees; distances in Å.

in a cis fashion with an O(1)−Sn−O(2) angle of 82.81(10)°. The two phosphoramide units are nearly identical; therefore, for simplicity, the structural parameters for only one phosphoramide unit are described. Some of the more important parameters are summarized in Table 2. The external nitrogens on the linker N(3) and N(6) are almost planar (∑N(3) = 359.4(9)°). The carbon atoms C(1) and C(5) on the linker are nearly eclipsed with the oxygen of the phosphoramide (torsional angle O(1)−P(1)−N(3)−C(1) = 2.3(4)°). The P(1)−O(1)−Sn vector adopts a 144.62(16)° bend. The tin atom is canted away from the linker and is located close to the diazaphospholidine ring (torsional angle Sn−O(1)−P(1)−N(3) 160.7(3)°). The nitrogens in the diazaphospholidine ring are pyramidalized as a result of ring strain (∑N(1) 350.5(8)°, ∑N(2) 350.8(8)°), and the direction of pyramidalization follows from the influence of the chiral backbone such that the methyl groups are cis to the hydrogens. Finally, it is interesting that the methylene subunits in the tether occupy a nicely staggered *syn*-pentane alignment (Figure 5b).

To further improve the enantioselectivity of the allylations with **1**, we surveyed several other dimeric phosphoramides with various chiral diamines as subunits. Among these, the bisphosphoramide **7d** based on (*R*,*R*)-2,2′-bispyrrolidine turned out to be the most selective catalyst in the allylation reaction. Accordingly, to provide an understanding of the special features

(15) (a) The crystallographic coordinates of **5d**·$SnCl_4$ have been deposited with the Cambridge Crystallographic Data Centre; deposition no. CCDC 164277. (b) *S*-(*l*,*l*)-**7d** was employed in the solid-state study. For convenience, the image of *R*-(*l*,*l*)-**7d**·$SnCl_4$ is shown. The crystallographic coordinates of *S*-(*l*,*l*)-**7d**·$SnCl_4$ have been deposited with the Cambridge Crystallographic Data Centre; deposition no. CCDC 195247. (c) The crystallographic coordinates of **7c**·$SnCl_4$ have been deposited with the Cambridge Crystallographic Data Centre; deposition no. CCDC 195246. These data can be obtained free of charge via www.ccdc.cam.ac.uk/conts/retrieving.html (or from the Cambridge Crystallographic Data Centre, 12 Union Road, Cambridge CB2 1EZ, U.K.; fax: (+44) 1223-336-033; or deposit@ccdc.cam.ac.uk).

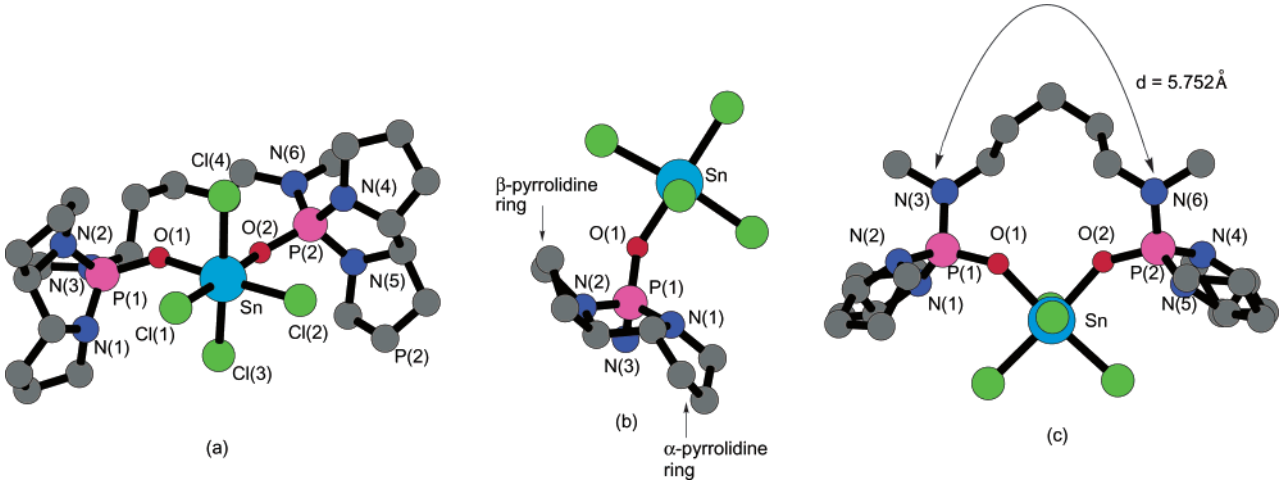

Figure 6. Chem 3D image of **7d**·$SnCl_4$ (hydrogens omitted for clarity).

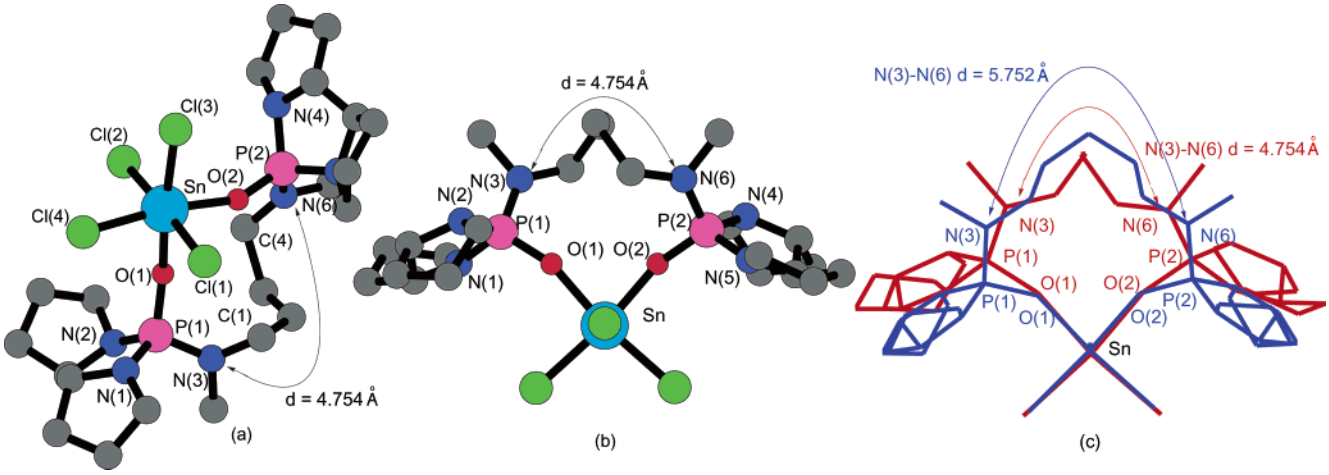

Figure 7. Chem 3D image **7c**·$SnCl_4$ (hydrogens omitted for clarity).

of **7d**, we sought to investigate its structure and conformational properties in the solid state.

Thus, slow diffusion of pentane into a solution of equimolar amounts of **7d** with $SnCl_4$ in CH_2Cl_2 provided single crystals suitable for X-ray diffraction analysis.[15b] In this complex (Figure 6 and Table 2), the tin atom adopts an octahedral geometry with bisphosphoramide chelated in a cis manner (angle O(1)−Sn−O(2) 84.87(13)°) as was seen in the **5d**·$SnCl_4$ complex. The basic structural characteristics of the diazaphospholidine rings and tether in **7d**·$SnCl_4$ are similar to those in **5d**·$SnCl_4$. The Sn−O(1)−P(1) angle is 140.99(15)°, and the torsional angle O(1)−P(1)−N(3)−C(1) is 6.8(4)°. The tin atom again is positioned above the five-membered rings of the phosphoramides (torsional angle Sn−O(1)−P(1)−N(3) −137.1(2)°).

The nitrogens in the diazaphospholidine ring are again pyramidalized (∑N(1) 349.5(10)°, ∑N(2) 354.4 (9)°). More importantly, due to the linkage of the substituents on the nitrogens to the backbone, the two pyrrolidine rings adopt a stairlike geometry, creating a highly asymmetric environment. As shown in the side view (Figure 6b), this chiral space directly influences the disposition of the tin atom. To avoid steric interactions with the β-pyrrolidine ring, the tin atom tilts away toward the α-pyrrolidine. This deformation in response to the ligand as a result of the chiral environment is correspondingly manifested in the relatively smaller Sn−O(1)−P(1)−N(3) torsional angle (−137.1(2)°) than that in **5d**·$SnCl_4$ complex (torsional angle Sn−O(1)−P(1)−N(3) 160.7(3)°).

As shown in Figure 2, the four-methylene-tethered bisphosphoramides **5c** and **7c** provided low selectivities in the allylation reaction as compared to **5b**, **5d**, and **7d**. To provide insight into how the deletion of one CH_2 group could have such a profound effect, we investigated the **7c**·$SnCl_4$ complex. Single crystals suitable for X-ray diffraction analysis were obtained from a solution of an equimolar mixture of **7c** and $SnCl_4$ in $CHCl_3$ by slow diffusion of pentane.[15c] In this complex as well, the tin atom adopts an octahedral geometry with **7c** chelating in a cis fashion (angle O(1)−Sn−O(2) 81.3(5)°) (Figure 7 and Table 2). The structure of the phosphoramide moiety is similar to that in the **7d**·$SnCl_4$ complex. The nitrogens N(1) and N(2) in the diazaphospholidine ring are pyramidalized (∑N(1) 353.7(32)°, ∑N(2) 345.0(31)°), and the nitrogen N(3) on the linker is nearly planar (∑N(3) 359.9(30)°). As before, the carbon on the linker C(1) is nearly eclipsed with the oxygen on the phosphoramide.

However, in this complex, due to the shorter tether length, several differences from the **7d**·$SnCl_4$ complex are noticeable. As shown in Figure 7b, the direct distance between the two linker nitrogens in this complex (4.754 Å) is significantly shorter as compared to that in the **7d**·$SnCl_4$ complex (5.752 Å) (Figure 6c and Table 2). Such a short tether length results in a larger

Sn−O(1)−P(1) (153.3(8)° vs 140.99(15)° in **7d**·$SnCl_4$) and a smaller Sn−O(1)−P(1)−N(3) torsional angle (−109.9(15)° vs −137.1(2)° in **7d**·$SnCl_4$). These differences are readily seen in the superposition of **7c**·$SnCl_4$ and **7d**·$SnCl_4$ in Figure 7c.

These X-ray crystal structures provided a wealth of information about the detailed molecular environment around the central tin atoms. The geometrical consequences of orienting each phosphoramide unit around the tin atom within the restrictions imposed by the connecting tether critically influence the spatial features of the reaction field. A clearer understanding of these details now supports the correlation of catalyst structure and selectivity as discussed below.

Discussion

1. Solution Structure of Complexes. The observation of stable unique structures in solution provided very important information on the behavior of the bidentate bisphosphoramides with a Lewis acid. In solution, only triplet signals with chemical shifts ranging from −706 to −725 ppm were observed in the ^{119}Sn NMR spectra, and, in most cases, the ^{31}P NMR spectra also displayed satellite signals with coupling constants similar to those in the ^{119}Sn NMR signals. The appearance of triplets due to the $^{119}Sn-^{31}P$ coupling suggested the coordination of two phosphoramide units to the tin center. Because the chemical shifts of the signals agree well with a hexacoordinate tin species, these complexes can be assigned as octahedral two-phosphoramide·$SnCl_4$ complexes.

The hexacoordinate tin species formed in solution are quite different depending on the concentration and the structure of phosphoramides. In the case of monophosphoramide **4**, two triplet signals were observed in a solution containing a 2/1 mixture of **4** and $SnCl_4$, and the coupling constants of the two triplets agreed well with the coupling constant range for *cis*- and *trans*-coordinated complexes.[13,14] Thus, it was concluded that both the *cis*- and the *trans*-complexes are present in solution and the energy difference between the *cis*- and *trans*-complexes is quite small.

The ^{119}Sn NMR spectra of equimolar mixtures of bisphosphoramides and $SnCl_4$ were highly dependent on the tether and concentration. At 0.20 M, bisphosphoramides **5c**, **5d**, **7c**, and **7d** tethered with four or five methylene units displayed only one triplet signal, which was different from the (monophosphoramide)$_2$·$SnCl_4$ complex. The difference between the observation of two complexes (cis and trans) with monophosphoramide and a single complex with bisphosphoramides **5c**, **5d**, **7c**, and **7d** at the same concentration strongly supported the hypothesis that the latter exist as chelates. Furthermore, the relatively small coupling constants observed for these ^{119}Sn triplets further suggested the presence of *cis*-chelated complexes in solution, which was consistent with the solid-state X-ray analysis of the **5d**·$SnCl_4$, **7c**·$SnCl_4$, and **7d**·$SnCl_4$ complexes.

At high concentration (0.20 M), the ^{119}Sn NMR spectrum of equimolar mixtures of bisphosphoramides **5b**, **5e**, and **7e** with $SnCl_4$ showed more than one triplet signal. Presumably, because of either the structural restriction (**5b**) or the greater entropy loss (**5e**, **7e**), the formation of chelated complexes was not as favorable. Instead these potentially chelating bisphosphoramides functioned as monodentate ligands and formed hexacoordinate oligomeric tin complexes involving two independent molecules of the bisphosphoramide (Figure 8).

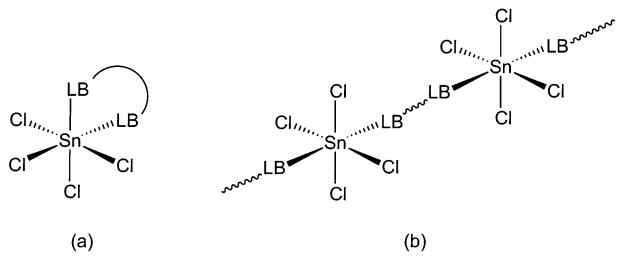

Figure 8. Competition between *cis*-chelated bis-phosphoramide·$SnCl_4$ complex (a) and *trans*-coordinated bis-phosphoramide·$SnCl_4$ oligomer (b).

In addition, the formation of an oligomeric complex with two phosphoramides coordinated to $SnCl_4$ would be favored at higher concentration, while the intramolecular *cis*-chelated complex would be preferred at lower concentration. The dependence of complexation on the concentration was clearly manifested in the spectra of equimolar mixtures of **5b** or **5e** and $SnCl_4$. As shown in Table 1, a 0.20 M solution containing a 1/1 mixture of **5b** and $SnCl_4$ displayed two triplets, a major one at −725 ppm with a coupling constant of 192 Hz and a minor one at −711 ppm with a coupling constant of 150 Hz. At lower concentration, the signal at −725 ppm disappeared, and only the triplet at −710 ppm with a coupling constant of 157 Hz was seen. The exclusive formation of one species at lower concentration suggested a chelated bisphosphoramide·$SnCl_4$ complex. In addition, due to the small magnitude of the coupling constant, this species could be assigned as a *cis*-chelated **5b**·$SnCl_4$ complex. While at higher concentration, the major signal has a coupling constant of 192 Hz, indicating a *trans*-coordinated phosphoramide·$SnCl_4$ complex. Because it is geometrically impossible for the ligand to chelate in a trans fashion due to the short tether length, the major triplet signal is assigned to a *trans*-coordinated oligomeric tin complex involving two phosphoramides (Figure 8b).

The effect of the concentration on the signals in the ^{119}Sn NMR spectrum was also observed for equimolar solutions of **5e** and $SnCl_4$. At higher concentration (0.20 M), the major triplet signal at −724 ppm had a coupling constant of 208 Hz, while at lower concentration, the spectrum displayed only a triplet at −710 ppm with a 113 Hz coupling constant. The dependence of the ^{119}Sn NMR spectra on the concentration strongly suggested the competition between the formation of chelated and nonchelated complexes. Thus, at higher concentration, an oligomeric *trans*-coordinated, phosphoramide·$SnCl_4$ complex[16] was preferentially formed, while the *cis*-chelated complex was favored at lower concentration.

Finally, an equimolar solution of **5a** and $SnCl_4$ shows a triplet with a large coupling constant of 182 Hz at even lower concentration (0.015 M), which suggested that the two phosphoramide units coordinate in a trans manner in the hexacoordinate tin complex. As mentioned before, a *trans*-chelated complex is structurally forbidden. Thus, this signal was assigned as a *trans*-coordinated oligomeric tin complex involving two independent phosphoramide units. Clearly, the two-methylene-unit tether was too short for **5a** to form a chelated complex with $SnCl_4$, and instead it rather functions as a monodentate ligand. Upon coordination of one phosphoramide unit to the

(16) Although two independent bisphosphoramide molecules are bound to tin, the net stoichiometry remains 1/1 because of the oligomeric nature of the complex. No free $SnCl_4$ was observed in the ^{119}Sn NMR spectrum.

tin atom, the appended phosphoramide unit functions as a large substituent; thus, the bisphosphoramide **5a** can be viewed as a bulky monodentate phosphoramide.

2. Implications of Bisphosphoramide·$SnCl_4$ Complexes in the Allylation Reaction. The ^{119}Sn NMR spectroscopic studies strongly supported the ability of bisphosphoramides to function as bidentate ligands. The propensity for chelation, however, was highly dependent on concentration and tether length. The observation of different complexes in solution together with selectivity observed in the allylation reaction provided the foundation of our hypothesis for the mechanism of this process.

First, the spectroscopic analysis demonstrated that bisphosphoramide **5a** can be considered as a bulky monodentate phosphoramide instead of a chelating bisphosphoramide. In the allylation promoted by **5a**, the product was obtained in racemic form. Because our previous studies on the allylation reaction have revealed that sterically bulky phosphoramides gave poor enantioselectivity,[6a] the low selectivity was presumably due to the steric bulk of this monodentate phosphoramide.

Second, although **5b** and **5e** could form chelated complexes with $SnCl_4$ at lower concentration as judged by ^{119}Sn NMR studies, caution must be taken when extrapolating these observations to the results of the allylation, in which the silicon is the organizational center. Furthermore, the results from bisphosphoramides **5** were obtained under high promoter concentration (0.50 M). In the allylation reaction, these two catalysts provide selectivities rather similar to those of the monophosphoramide; therefore, it is more likely that these ligands behave as monodentate ligands in the reaction as well.

Third, catalysts **5c**, **7c** and **5d**, **7d** bearing four and five methylene units are found to be ideal for chelation of phosphoramides, as evidenced in the exclusive formation of single complexes with $SnCl_4$, even at high concentration. The chelation, however, does not necessary lead to an enhanced enantioselectivity as compared to the monophosphoramide. In the allylation reaction, whereas bisphosphoramides **5d**, **7d** with five methylene units gave higher selectivities than the monophosphoramides, poor selectivities were observed in the reaction catalyzed by bisphosphoramides **5c**, **7c** tethered with four methylene units. The lower selectivities observed with **5c**, **7c** might have their origin in the unfavorable arrangement of the phosphoramide groups due to the dictates of the tether length and flexibility, which will be addressed below in the structural studies.

Finally, although monophosphoramide **4** formed both *cis*- and *trans*-2/1 hexacoordinate complexes with $SnCl_4$, it was not clear whether the transition structure in allylation reaction would involve both *trans*- and *cis*-positioned phosphoramides. This ambiguity on the orientation of two phosphoramides certainly complicates the analysis of the allylation reaction promoted by monophosphoramides and bestows an added benefit of using bisphosphoramides because only *cis*-chelated complexes can possibly be formed.

3. Conformational Information from X-ray Structures of Complexes of Bisphosphoramides with $SnCl_4$. The solid-state X-ray crystal structure analysis of **5d**·$SnCl_4$, **7c**·$SnCl_4$, and **7d**·$SnCl_4$ complexes provided detailed information on their coordination geometry, which provided a structural basis for understanding the origin of different selectivities in allylation reactions.

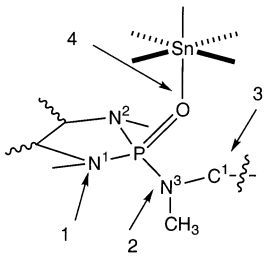

Figure 9. Common features in phosphoramide·$SnCl_4$ complexes.

In these complexes, there are several structural characteristics that are preserved throughout the series (Figure 9): (1) the nitrogens in the diazaphospholidine rings are pyramidalized, (2) the nitrogens on the linker are nearly planar, (3) the plane containing the external nitrogen is perpendicular to the diazaphospholidine ring, and the carbon atoms on the linker are nearly eclipsed with the oxygen of the phosphoramide, and (4) to avoid possible steric interactions, the tin atoms turn away from the tether and are positioned above the diazaphospholidine ring.

The detailed location of the tin atom with respect to the phosphoramide moiety, however, is highly dependent on the chiral diamine and tether length (Figure 10). First, because the tin atom is in close proximity to the chiral diamine, its disposition directly reflects the asymmetric environment imposed by the chiral diamine. In the **5d**·$SnCl_4$ complex, the methyl groups and the backbone skeleton are trans to each other; thus, they might have opposite influences on the asymmetric induction. Because of the ill-defined chiral environment, the location of the tin atom is rather unbiased with respect to the diazaphospholidine ring (torsional angle Sn−O(1)−P(1)−N(3) 160.7(3)°). In the **7d**·$SnCl_4$ complex, the stairlike geometry of the bispyrrolidine rings creates a highly asymmetric environment. This defined chiral space causes the tin atom to stay away from the pyrrolidine ring and results in a smaller torsional Sn−O(1)−P(1)−N(3) angle (−137.1(2)°).

Second, the influence of the tether length on the coordination geometry of the bisphosphoramide·$SnCl_4$ complex was apparent by comparing the **7c**·$SnCl_4$ with **7d**·$SnCl_4$ complexes. The shorter tether resulted in a larger Sn−O(1)−P(1) angle (153.3(8)°) (Figure 7c) and a smaller Sn−O(1)−P(1)−N(3) torsional angle (−109.7(15)°) (Figure 10c). In addition, our previous studies on the monophosphoramide·$SnCl_4$ complexes have revealed that the torsional angle Sn−O(1)−P(1)−N(3) has a range from 135 to 178°. In this case, to accommodate the four methylene tether, the Sn−O(1)−P(1)−N(3) angle was also significantly smaller than those in the free monophosphoramide·$SnCl_4$ complexes. The influence of tether length on the coordination geometry provided an explanation for why bisphosphoramides with shorter tethers would be less likely to form chelated complexes with $SnCl_4$.

4. Transition Structure Assembly in Allylation Reactions. With the detailed structural information provided by the X-ray studies, it is possible to formulate transition structure models for the allylation reaction catalyzed by **7d**. The geometry of the bisphosphoramide and silicon in the proposed cationic hexacoordinate siliconate transition structure could be deduced from the X-ray structure of **7d**·$SnCl_4$. An important issue regarding the transition structure is the coordination sites of the aldehyde and the allyl group with respect to the phosphoryl groups. In the allylation reaction, it is likely that the allyl

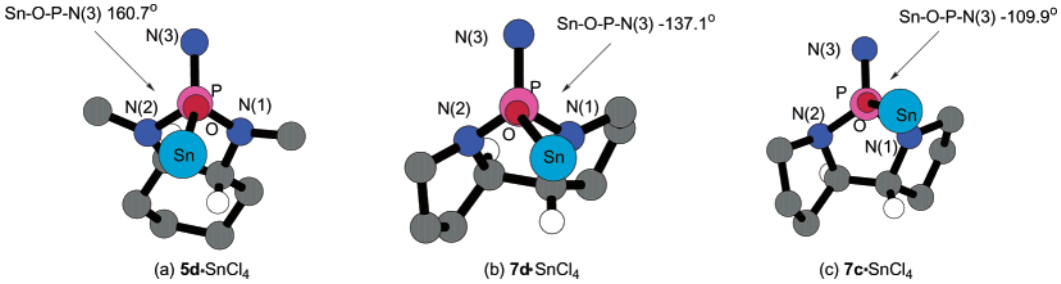

Figure 10. Comparison of different Sn−O−P−N(3) torsional angles.

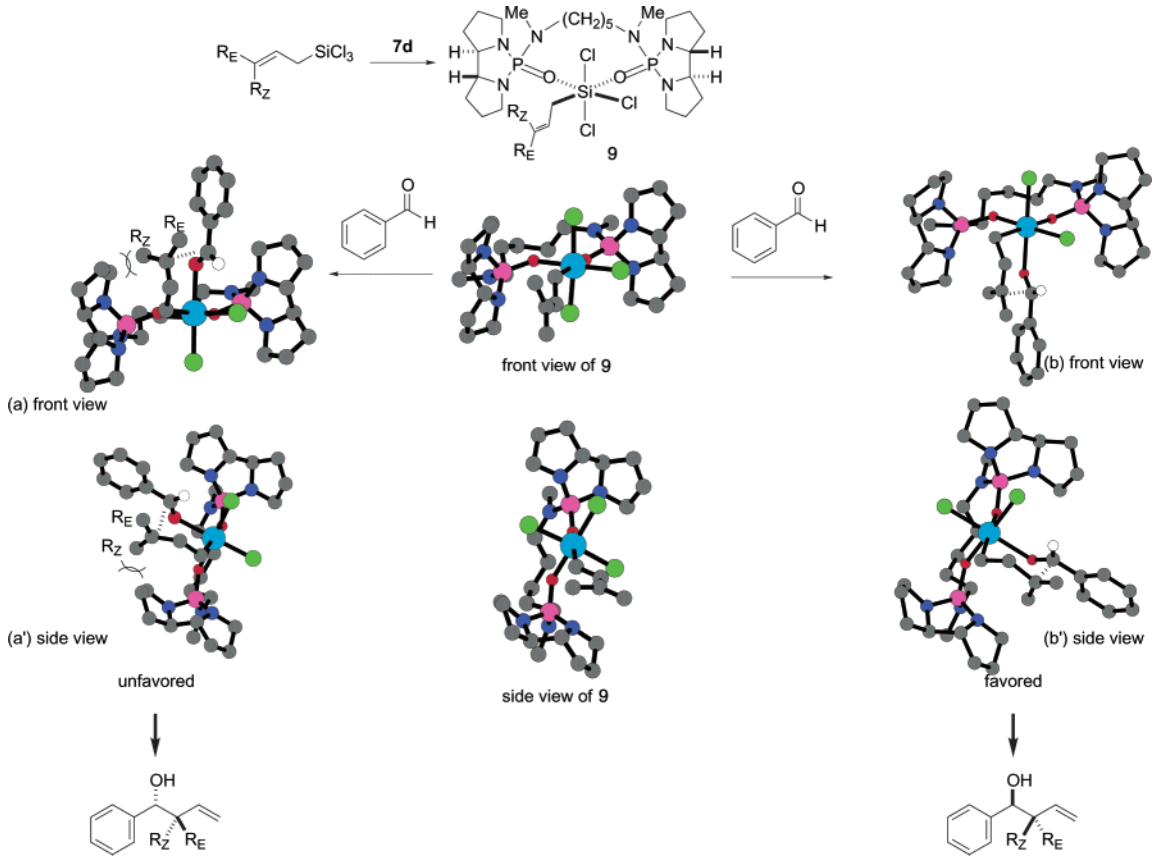

Figure 11. Hypothetical transition structures for allylation of benzaldehyde catalyzed by **7d**.

addition rather than any of prior step is rate-determining.[17] Accordingly, in the transition structure, the allyl group would be trans to one of the phosphoramides, rendering it more nucleophilic; at the same time, the aldehyde would coordinate trans to chloride to increase its electrophilicity.[18,19]

Given these assumptions, we composed a hexacoordinate allyltrichlorosilane bisphosphoramide complex **9** from the structure of **7d**·$SnCl_4$ by replacing one of the chloride ions trans to the phosphoramide unit with an allyl group (Figure 11). In this complex, the allyl group is in close proximity to the highly asymmetric stairlike phosphoramide moiety (Figure 11, front view and side view). From this complex, ionization of one chloride anion and coordination of the aldehyde generates the reactive complex, which then reacts through a chairlike transition structure.[6] In one of the possible chairlike transition structure assemblies (Figure 11a, 11a′), the allyl group, especially the *Z*-substituent on the allylic silane, is in close proximity with the *β*-pyrrolidine ring. Such steric interaction does not exist in the other arrangement (Figure 11b, 11b′), because the α-pyrrolidine ring is oriented below the diazaphospholidine ring. On the basis of this analysis, we propose that the reaction with *R*-(*l*,*l*)-**7d** proceeds through a transition structure similar to that shown in Figure 11b, leading to the observed homoallyl alcohol of *S*-configuration at the hydroxyl center. The strong interaction between the *Z*-substituent and the *β*-pyrrolidine ring also explains the beneficial effect of the *Z*-substituent on the enantioselectivity observed in *syn*-crotylation and prenylation reactions.[6c]

(17) In chiral Lewis base-catalyzed aldol reactions, kinetic isotope effect studies revealed that the rate-determining step is the addition of the nucleophile to complexed aldehyde: Pham, S. M.; Bui, T., unpublished results from these laboratories.

(18) Reviews on the reactivity of hypercoordinate silicon compounds: (a) Kost, D.; Kalikhman, I. In *The Chemistry of Organic Silicon Compounds*; Rappoport, Z., Apeloig, Y., Eds.; Wiley: Chichester, 1998; Vol. 2, Part 2, pp 1339. (b) Holmes, R. R. *Chem. Rev.* **1996**, *96*, 927. (c) Chuit, C.; Corriu, R. J. P.; Reye, C.; Young, J. C. *Chem. Rev.* **1993**, *93*, 1371. (d) Tandura, S. N.; Voronkov, M. G.; Alekseev, N. V. *Top. Curr. Chem.* **1986**, *131*, 99.

(19) Reviews on the trans effect and ligand donor abilities: (a) Coe, B. J.; Glenwright, S. J. *Coord. Chem. Rev.* **2000**, *203*, 5. (b) Appleton, T. G.; Clark, H. C.; Manzer, L. E. *Coord. Chem. Rev.* **1973**, *10*, 335.

Finally, the lower enantioselectivity observed with **7c** as compared to **7d** in allylation can be understood considering the coordination geometry of the **7c**·$SnCl_4$ complex provided by X-ray crystallography. First, as compared to **7d**·$SnCl_4$, **7c**·$SnCl_4$ possesses a larger Sn−O(1)−P(1) angle, which suggests a more open chiral space and a diminished influence of the chiral skeleton on the reaction center. Second, the smaller torsional angle Sn−O(1)−P(1)−N(3) indicates that the tin atom is positioned away from the β-pyrrolidine ring. Because we invoked that the unfavorable transition structure arose from the interaction between the allyl group and the β-pyrrolidine ring, an increased distance between these two moieties certainly decreased the interaction, leading to the lack of stereocontrol.

These studies clearly demonstrate how a deletion of one methylene unit can influence the coordination geometry of the complex and lead to a dramatically decreased enantioselectivity. A five-methylene-unit tether was not only important for chelation but also necessary to bring the chiral information close to the reaction center, achieving high asymmetric induction. The special coordination geometry associated with five-methylene-tethered bisphosphoramides also provided an understanding for their selectivities, which are higher than those of bisphosphoramides with other tethers, regardless of the chiral diamine backbone employed.

Conclusion

Solution NMR spectroscopic and X-ray crystallographic studies provided crucial insight into the behavior of bisphosphoramides when complexed with a Lewis acid. The formation of chelated complexes with $SnCl_4$ was strongly supported by ^{119}Sn NMR analysis in solution and X-ray analysis in the solid state. However, the extent of chelation versus complexation was highly dependent on the solution concentration and the tether length. These observations agreed well with the influence of concentration and tether length on the enantioselectivity in the allylation promoted by bisphosphoramides. The solid-state structures also provided detailed information on factors influencing the chelate formation as well as the coordination geometry of the bisphosphoramide·$SnCl_4$ complexes. The unique features of **7d** are its ability to function as bidentate ligand, to bring the chiral environment close to the reaction center, and the highly asymmetric environment created by the bispyrrolidine backbone. Further kinetic studies to support the transition structure assembly as well as the design of more selective and general bisphosphoramide catalysts for trichlorosilane chemistry are under investigation.

Acknowledgment. We are grateful for the National Science Foundation for generous financial support (NSF CHE 9803124 and 0105205). We thank Dr. Scott R. Wilson for the assistance with crystal structures. J.F. thanks the Boehringer Ingelheim Pharmaceutical Co. for a graduate fellowship.

Supporting Information Available: Description of the solution NMR experiments and the structure determination of **5d**·$SnCl_4$, **7c**·$SnCl_4$, **7d**·$SnCl_4$, and tables of crystallographic data (PDF). This material is available free of charge via the Internet at http://pubs.acs.org.

JA021280G